

Distribution of Cathode Current Density and Breaking Capacity of Medium Voltage Vacuum Interrupters with Axial Magnetic Field

S.M. Shkol'nik², V.P. Afanas'ev², Yu.A. Barinov², A.M. Chaly¹,
A.A. Logatchev², S.I. Malakhovsky¹, I.N. Poluyanova¹, K.K. Zabello²

¹IG Tavrida Electric, 1, Biryuzova, Moscow, 123298, Russia

²A.F. Ioffe Phys.- Techn. Institute, Rus. Acad. Sci., 26, Polytechnicheskaya, St.-Petersburg, 194021, Russia

Abstract - Earlier we offered technique of high-speed photography of high-current vacuum arc that in combination with the special computer-aided treatment allowed reconstruction of distribution of current density on the cathode. This technique was applied for butt solid contacts with external axial magnetic field (AMF) at relatively low current density $j < 2 \text{ kA/cm}^2$. In the present work we have further developed this technique. Advanced technique is applicable for the analysis of current density distribution on the complicated electrodes of commercial vacuum interrupter (VI) carrying current up to $I = 50 \text{ kA}$ at current density up to $j \sim 4 \text{ kA/cm}^2$. The experiments have been carried out for three types of electrode systems generating AMF with different configurations. The obtained results proved previously derived conclusion that current density tends to distribute evenly across that part of the contact surface where AMF induction fits inequity $B_z^{(1)} < B_z < B_z^{(2)}$, where $B_z^{(1)}$, $B_z^{(2)}$ - characteristic inductions defined in our previous work. Slots on the electrode surface lead to substantial non-uniformity of current density distribution even if AMF is properly configured. Comparison of breaking capacity and distribution of current density for different electrode systems proves that interruption failure occurs at peak current density $\sim 3.5 \text{ kA/cm}^2$. This value exceeds by at least 50% maximum current density interruptible by commercial VI. We have also found out that changing configuration of AMF may substantially improve breaking capacity: in our experiments slide modification of AMF distribution provides 12% increase of breaking capacity.

INTRODUCTION

Stabilization of arc discharges with the aid of axial magnetic fields (AMF) is an established and prevalent method for improvement performance of various discharge devices [1, 2]. In the course of research of high-current vacuum arcs (HCVA), carried out in view of improvement of vacuum interrupters (VI), this method has been successfully used and provided remarkable increase of VI breaking capacity [3, 4].

Free burning HCVA is inherently unstable. This instability is determined by retrograde movement of cathode spots (CS) under the effect of the self-magnetic field of the arc current [5]. Due to this movement area occupied by CS (cathode arc attachment) expands after arc ignition until substantial fraction of CS leaves front contact surface and appears on its

lateral surface. This provides extra loss of ions, which in its turn, creates conditions necessary for development of arc instability and transition from diffuse to constricted mode (refer to [6,7] for more details). This transition limits breaking capacity of free burning HCVA by $\sim 10 \text{ kA}$.

Application of AMF dramatically affects dynamics of CS preventing them from leaving front contact surface [8]. AMF also narrows CS plasma jets [9] reducing radial losses of ions providing additional stabilization of HCVA. These effects hamper constriction of HCVA and result in appropriate growth of VI's breaking capacity.

At the same time it is clear that this growth cannot be unlimited. At a certain current level, even if the arc is restrained by AMF in the diffuse mode, surface temperature of the former anode becomes too high, producing enough vapour to facilitate breakdown across contact gap after current zero crossing. Breakdown mechanism is not clearly understood today, however, one can reasonably assume that for HCVA stabilized by AMF higher breaking capacity corresponds to the current being most uniformly distributed over the entire electrode surface.

For uniform AMF optimum current distribution in a quasi-stationary arc state is achieved when AMF induction is, on the one hand, sufficient to hold CS on the front cathode surface, and, from the other hand, not too high, so that it prevents CS from occupying the entire cathode surface [8]. For commercial VI AMF is generally substantially non-uniform. It has been shown in literature that AMF shape may affect distribution of current density significantly [10, 11]. However, to our knowledge, these observations were exclusively qualitative.

Gaining quantitative data on the current distribution in a HCVA is a complicated problem. Magnetic probes have been successfully applied for vacuum arcs with butt electrodes with currents of order of several kA [12]. At the same time electrodes of conventional VI operate at current equal to several tens of kA. This current will provide severe thermal stress on the magnetic probes, which may exceed their thermal stability. So, applicability of this technique is doubtful. Another problem is associated with the fact that conventional VI electrodes have slots and therefore have axial symmetry of a relatively low order. Numerous measurements

will be required to restore the two-dimensional picture of the current density distribution.

High speed filming remains up to now the main technique for obtaining information on the current distribution in a HCVA. Modern hardware allows simultaneous filming in two directions [13]. However, at the present stage of the vacuum arc theory only qualitative relation of the distribution of radiation intensity from the arc column and arc current distribution is possible.

The same is true with regard to technique using erosion imprints.

In [14] we offered technique of high-speed photography of HCVA cathode surface that in combination with the special computer-aided treatment allowed reconstruction of distribution of current density on the cathode. This technique has been applied for butt solid contacts with external AMF. Later we successfully applied this technique for special electrodes with self-generated AMF. This investigation allowed us finding optimum configuration of AMF [15].

The goals of the present study are as follows:

- Investigate possibility of application of this technique for electrodes of commercial VI
- Investigate distribution of current density on electrodes of commercial VI
- Investigate possibility to influence distribution of current density with the aid of configuration of AMF
- Compare results related to distribution of current density with the breaking capacity tests.

II. EXPERIMENTAL HARDWARE AND PROCEDURE

The experiments were carried out for three types of electrode systems (N1, N2 and N3) generating AMF with different configurations. Contact plates were manufactured from copper-chromium composition. Contacts had radial slots for eddy currents suppression (Fig. 1).

The experiments were performed in a demountable vacuum chamber under continuous pumping, providing pressure $\sim 10^{-4}$ Pa. The block diagram of the experimental setup is shown in Fig. 2. Interelectrode gap was fixed at $h=4$ mm. The discharge was ignited on the cathode surface at a distance ≈ 8 mm from the edge using molybdenum needle. The discharge was powered from a special generator providing rectangular current pulse with adjustable current up to 50 kA

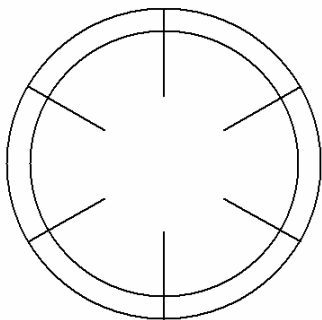


Fig. 1. Front view of electrode (schematically).

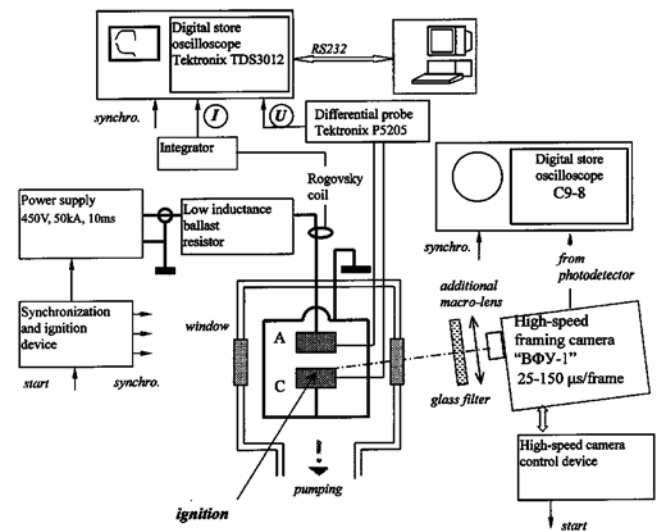


Fig. 2. Block diagram of the experimental setup.

and duration up to 10 ms. Prior to measurements, the cathode surface was cleaned with a set of high-current pulses.

Discharge current and voltage were measured with the aid of oscilloscope TDS3012. The voltage was measured with differential probe P5205 connected directly to the reverse side of the contacts. The current was measured with Rogovsky coil. Transmission band for current measurement was equal to ~ 1 MHz.

The cathode surface was photographed using high-speed photography (HSP) camera. The camera allowed capturing 60 sequential frames during current pulse. The start of filming could be delayed by 0-5 ms. Exposure of frame could be varied within wide limits. This allowed filming the entire pulse first and then, with higher time resolution, selected intervals. Camera axis was inclined by $\sim 10^0$ with regard to cathode surface. A red light filter was used to suppress plasma radiation and to improve contrast of the CS images.

Breaking capacity tests were conducted using double-synthetic circuit, providing IEC specified TRV with voltage peak 20 kV. Three types of VI (having the same electrode systems as the ones investigated with the aid of high speed photography) were manufactured and subjected to breaking capacity tests. VI contacts were driven with the aid of magnetic actuator used for commercial VCB. "Up and down" test method had been used in order to define maximum breaking capacity.

III. TECHNIQUE OF IMAGE PROCESSING AND DETERMINATION OF CURRENT DENSITY

Original technique applied for current density determination includes the following steps [14]:

- capturing cathode image with the aid of high speed camera;
- reconstruction positions of cathode spots;
- determination of current density (as density of CS).

a)

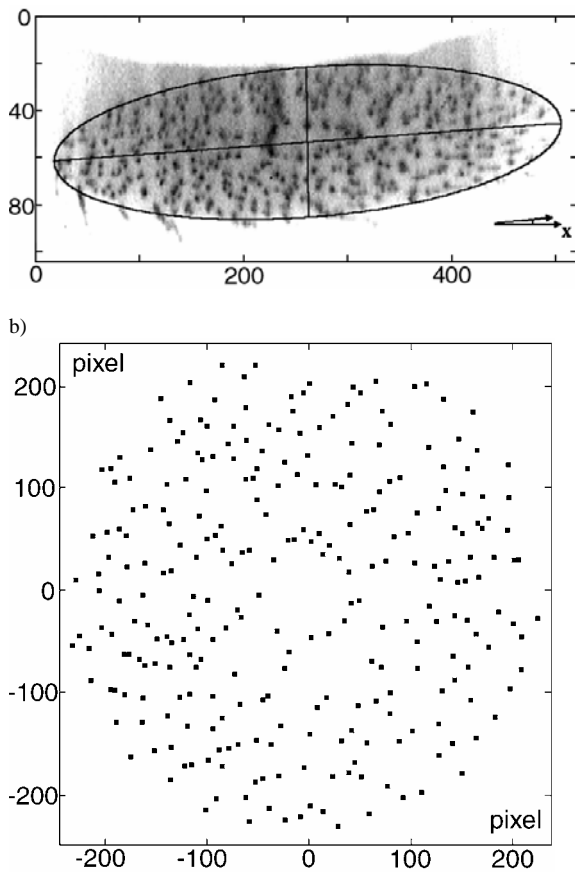


FIG. 3. Arc stabilized by a uniform axial magnetic field $I=11.3$ kA, $B=0.27$ T. Electrodes CuCr, diameter 30 mm, electrode gap 4 mm. a) HSP frame (negative, exposure $75 \mu\text{s}$) The ellipse marks the electrode edge (axis labels in pixels). The cathode is in the bottom. In the center one can see the ignition hole. b) Reconstructed cathode spots positions.

The first and the second step are illustrated in Fig. 3. It gives an example of processing result for a frame of the arc with relatively low average current density $j \sim 1.5$ kA/cm². This level of current density used to be close to the technique applicability limit in the past. The attempts of using the described procedure in the present work at higher current densities have shown the necessity to obtain images of a better quality and improve the processing technique. Application the up-to-date special fine-grain film with high resolution and large photographic latitude along with varying some filming parameters has allowed us obtaining satisfactory images of a discharge with high current density. Fig. 4 shows an example of filming of an arc in the electrode system N2 with current $I=45$ kA. Processing of such images required revision of the filtering algorithm, since, with a large number of cathode spots per film unit area, the structure of the images appeared to be very complicated.

For the last step Voronoy diagram has been applied in our previous work. This diagram relates each CS with the polygon. Each point of this polygon is located closer to the particular CS than to any other one. Then local current density has been calculated as a value inversely proportional to the

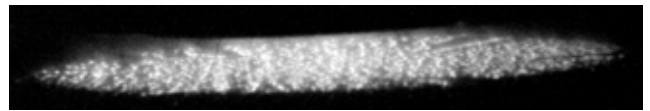


Fig. 4. HSP frame (positive, exposure $25 \mu\text{s}$) of the arc in the electrode system N2, $h=4$ mm, $I=45.4$ kA, the cathode is in the bottom.

square of the mentioned polygon. This method was successively applied for solid contacts with more or less uniform distribution of current density.

At the same time we found out that for electrodes of conventional VI current density may be distributed quite non-uniformly (Fig. 4). As one can see from this picture slots located on the contact surface disturb CS distribution. In this case Voronoy diagram may substantially distort actual current density.

To avoid this shortcoming we simulated current density as a superposition of functions $j = j_0 \cdot \exp(-4r^2/a^2)$, where r is the distance from the particular CS and a – conditioning parameter. We proved that variation of parameter a within reasonable limits provided a weak effect on computed current density.

One could assume that for relatively short vacuum arc in AMF (relevant for medium voltage VI) anode current density does not differ substantially from the cathode one. This assumption is supported with the comparison of erosion footprints on the cathode and on the anode presented in [16].

IV. EXPERIMENTAL RESULTS AND DISCUSSION

Fig. 5 presents typical oscillograms of arc current and voltage. As it follows from Fig. 5 current attained its quasi-stationary level in several hundred microseconds after arc ignition. At the same time stabilization of arc voltage was further delayed by 2-2.5 ms.

Computation of AMF evolution (Fig. 6) for current pulse corresponding to Fig. 5 proved that AMF established its quasi-stationary state in ~ 3 ms after arc ignition, due to eddy currents. On this basis we assumed that delay in stabilization of arc voltage was determined by delay in stabilization of AMF.

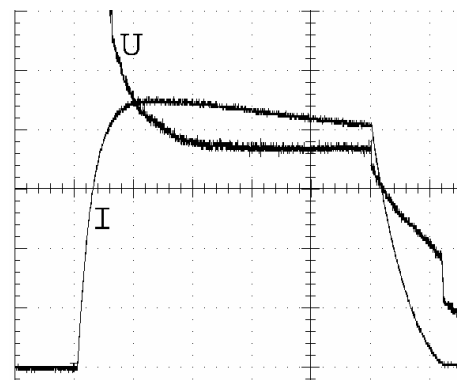


Fig. 5. Oscillograms of the arc current and voltage ($t-1$ ms/div, $I-10$ kA/div, $U-10$ V/div). Electrode system N1.

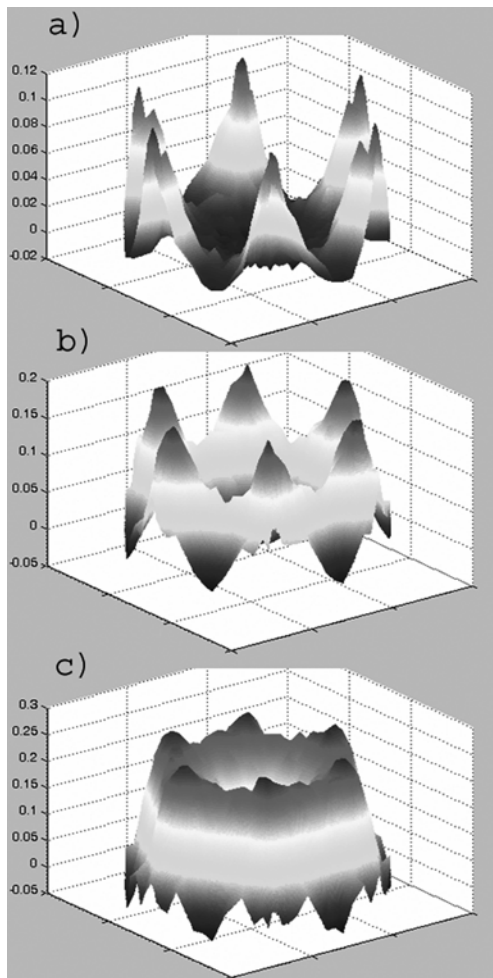


Fig. 6. AMF calculation results (electrode system N1). Current pulse shape is in correspondence with oscillogram in Fig. 5.

a) $t=0.2$ ms after arc ignition; b) $t=0.6$ ms; c) $t=3$ ms.

HSP-filming proved this assumption. In the initial stage after arc ignition CS occupied only peripheral area (where substantial AMF had been established). With the penetration of AMF into central area (in 2-3 ms after arc ignition) CS moved into it, establishing quasi-stationary state of the arc. This behavior complied with the “self-adjustment” of the arc to the momentary configuration of AMF observed in [15] for simple electrode configurations.

In the present work we were interested in quasi-stationary state of the arc. So, we performed HSP-filming of the arc for all three types of electrodes in 3.5 ms after arc ignition. Currents were varied from 25 to 45 kA and filming duration was fixed at 1.5 ms. This duration corresponded to the exposure time 25 μ s/frame.

Fig. 7 illustrates cathode image of the electrode system N1 at 35 kA current. Similar to Fig. 4 one can observe zones of CS concentration and rarefaction on the opposite sides of contact slots.

This effect is better distinguished in Fig. 8a presenting two-dimensional distribution of current density obtained with the aid of computing procedure described above. The two-

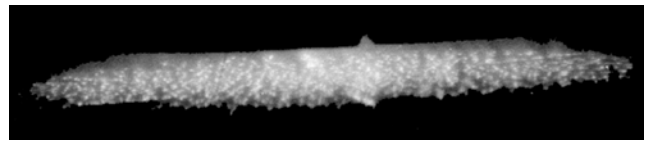


Fig. 7. HSP frame (positive, exposure 25 μ s) of the arc in the electrode system N1, $I=35$ kA, the cathode is in the bottom.

dimensional distribution of the current density, shown on Fig. 8a, is obtained by means of summarizing the results of processing of all 60 frames, fixed during a quasi-stationary state of the arc in single pulse.

Fig. 8b presents radial distribution of azimuthally averaged current density. Curves 1-3 are averaged within $0-360^\circ$. At this curve 1 is based on entire filming duration, while curves 2 and 3 - on the first and second halves of the filming duration correspondingly. Coincidence of all three curves proves, to our mind, consistency of the approach.

Fig. 8b also illustrates radial distribution of current density azimuthally averaged within the 30° sector located in the middle of contact petal (see Fig. 8a).

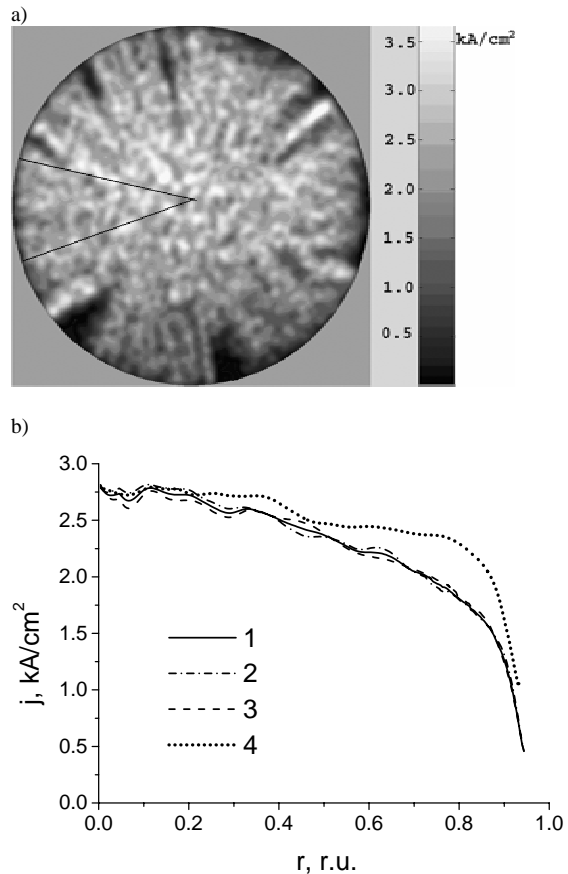


Fig. 8. The results of the treatment of arc images. Electrode system N1, $I=35$ kA.

a) two-dimensional distribution of the current density;
 b) azimuthally averaged ($0-360^\circ$) radial distribution of the current density - curves 1,2,3. 1 - summarizing over the whole filming; 2,3 - summarizing over the first and the second half of the filming; azimuthally averaged ($0-30^\circ$) radial distribution of the current density - curve 4. The position of the sector with the angle of 30° is shown in Fig. 8a.

As it can be seen from Fig. 8b averaged current density being nearly constant in the central area ($r < 0.4$) gradually decreases in the slotted peripheral area ($0.4 < r < 0.9$). At the same time current density decreases substantially slower for the sector located far from the slots (Fig. 8b). On this basis we conclude that contact slots are responsible for substantially non-uniform distribution of current density that shall provide negative effect on the breaking capacity of AMF electrodes.

For all curves we observed fast decrease of current density when contact radius exceeded ~ 0.9 . Computation of AMF induction at this point proved that it was approximately equal to characteristic value $B_z^{(1)}$, defined in [15]. This observation proves basic conclusions presented in [15]: if AMF configuration is convex, CS tend to occupy that part of the cathode surface where AMF induction B_z meets the condition $B_z^{(1)} < B_z < B_z^{(2)}$ ($B_z^{(2)}$ also is defined in [15]).

Fig. 9 illustrates normalized azimuthally averaged (within 0 to 360°) radial distributions of current density for electrode system N1 for different currents. It can be seen that, within the entire current range distribution of current density does not depend on current. To our mind it is natural result of the fact that generated AMF induction and its characteristic value $B_z^{(1)}$ are proportional to current.

Similar results were obtained for electrode systems N2 and N3. However, current distribution turned to be wider. The increase of the area occupied by CS on the cathode is, as the comparison of Fig. 11 and Fig. 10 shows, a consequence of growth in the size of the region where the induction of the AMF generated by electrode system exceeds the value of $B_z^{(1)}$.

Fig. 12 illustrates dependency of current density in the central not-slotted area on current for different electrode systems and their limiting interrupting currents. Current density had been computed on the basis of the present method. As it follows from Fig. 12 electrode system N3 demonstrated much better switching performance. It can also be seen that the limiting breakable current in various electrode systems examined in present experiment corresponds to roughly the same current density in the paraxial region of the

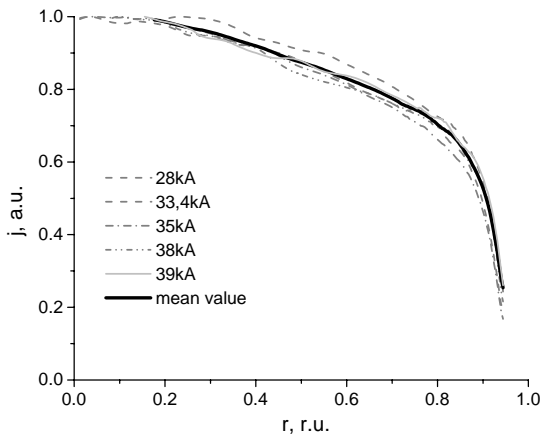


Fig. 9. Normalized radial distributions of current density (azimuthally averaged). Electrode system N1, currents are in between 28 and 39 kA.

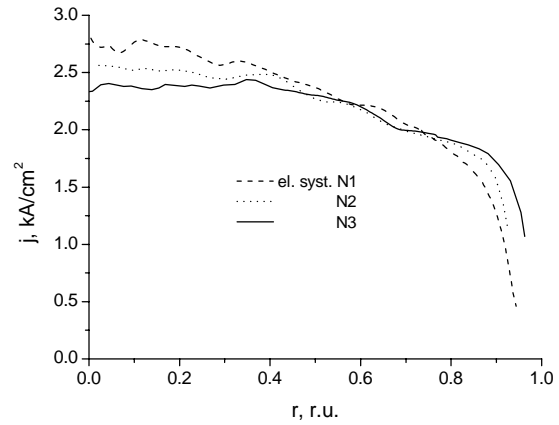


Fig. 10. Azimuthally averaged radial distributions of the current density of the arcs with $I=35$ kA in different electrode systems.

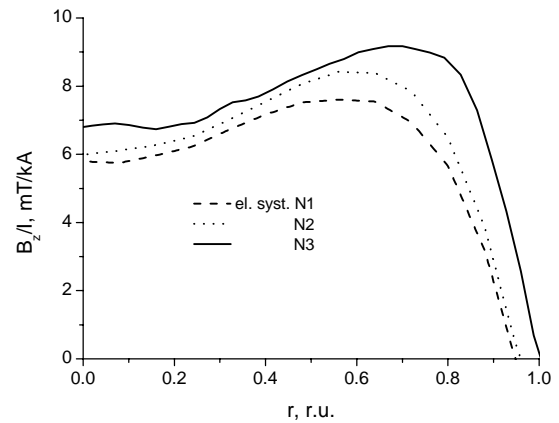


Fig. 11. Calculated radial distributions of the AMF induction in different electrode systems. The section across the middle of the contact petal.

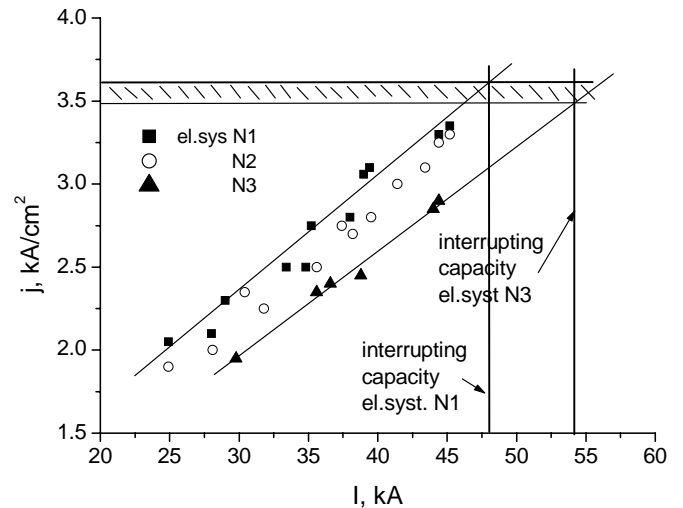


Fig. 12. Current density in the central not-slotted area versus current for different electrode systems and their limiting interrupting currents.

contact plate, $j \approx (3.5 - 3.6) \text{ kA/cm}^2$. This current density correlates well with the maximum interrupting current density estimated in [17].

V. CONCLUSION

The developed technique allows deriving two-dimensional distribution of current density in HCVA with a current of order of several tens of kA. This technique is applicable not only for butt solid contacts with external AMF, but also for commercial electrodes with non-uniform AMF. Application of this technique for these electrodes proved previously derived conclusion that current density in HCVA tends to distribute evenly across that part of the contact surface where AMF induction fits inequity $B_z^{(1)} < B_z < B_z^{(2)}$, where $B_z^{(1)}$, $B_z^{(2)}$ – characteristic inductions defined in [15].

We also discovered that slots on the contact surface lead to substantially non-uniform distribution of current density even if AMF is properly configured.

Comparison of breaking capacity and distribution of current density for different electrode systems proved that interruption failure in electrode systems examined in present experiments occurs at current density $j \approx (3.5-3.6) \text{ kA/cm}^2$. This value seems to be in good agreement with thermal estimation of maximum breaking capacity.

We also found out that changing configuration of AMF may substantially improve breaking capacity: in our experiments slide modification of AMF distribution provided 12% increase of breaking capacity.

REFERENCES

- [1] W. Finkelburg, "Hochstromkohlebogen," Berlin-Göttingen-Heidelberg, 1948.
- [2] G. Francis, "Ionization phenomena in gases," Butterworths scientific publications, London, 1960.
- [3] C.W. Kimblin and R.E. Voshall, "Interruption ability of vacuum interrupters subjected to axial magnetic fields," Proc. Inst. Elect. Eng., vol. 119, pp. 1754-1758, Dec. 1972.
- [4] S. Yanabu, S. Souma, T. Tamagawa, S. Yamashita, and T. Tsutsumi, "Vacuum arc under an axial magnetic field and its interrupting ability," Proc. Inst. Elect. Eng., vol. 126, pp. 313-320, Apr. 1979.
- [5] S.M. Shkol'nik, "Vacuum arc" in Encyclopedia of Low-Temperature Plasma, V.E. Fortov, Ed. Moscow, Russia: Nauka, 2000, vol. 2, pp. 115-132, (in Russian).
- [6] H.C. Miller, "A review of anode phenomena in vacuum arcs," Contrib. Plas. Phys., vol. 29, no. 3, pp.2233-2249, 1989.
- [7] S.M. Shkol'nik, "Secondary plasma in the gap of high-current vacuum arc: origin and resulting effects," IEEE Trans. Plasma Sci., vol. 31, no. 5, pp. 832-846, Oct. 2003.
- [8] A.M. Chaly, A.A. Logatchev, and S.M. Shkol'nik, "Cathode processes in free burning and stabilized by axial magnetic field vacuum arcs," IEEE Trans. Plasma Sci. vol. 27, no. 4, pp. 827-835, Aug. 1999.
- [9] W.G.J. Rondell, "The vacuum arc in axial magnetic field," J. Phys. D: Appl. Phys., vol. 8, no. 8, pp. 934-942, 1975.
- [10] B. Fenski, M. Heimbach, M. Lindmayer, and W. Shang, "Characteristics of a vacuum switching contact based on bipolar axial magnetic field," IEEE Trans. Plasma Sci., vol. 27, no. 4, pp. 949-953, Aug. 1999.
- [11] M. Homma, H. Somei, Y. Niwa, K. Yokokura, and I. Ohshima, "Physical and theoretical aspects of a new vacuum arc control technology – self arc distribution by electrode: SADE," IEEE Trans. Plasma Sci., vol. 27, no. 4, pp. 961-968, Aug. 1999.
- [12] M.S. Agarwal and R. Holmes, "Current flow-pattern in high-current metal-vapor arcs," in Proc. 7 Int. Conf. Gas Disch. Appl., London, U.K., 1982, pp.55-58.
- [13] W. Shang, E. Dullni, H. Fink, I. Kleberg, E. Scade, and D.L. Shmelev, "Optical investigations of dynamic vacuum arc mode changes with different axial magnetic field contacts," IEEE Trans. Plasma Sci., vol. 31, no. 5, pp.923-928, Oct. 2003.
- [14] V.P. Afanas'ev, A.M. Chaly, A.A. Logatchev, S.M. Shkol'nik, and K.K. Zabello, "Computer-aided reconstruction of cathode images obtained by high speed photography of high current vacuum arcs," IEEE Trans. Plasma Sci. vol. 29, no. 5, pp.695-699, Oct. 2001.
- [15] A.M. Chaly, A.A. Logatchev, K.K. Zabello, and S.M. Shkol'nik, "High current vacuum arc appearance in nonhomogeneous axial magnetic field," IEEE Trans. Plasma Sci. vol. 31, no. 5, pp.884-889, Oct. 2003.
- [16] A.M. Chaly, A.A. Logatchev, S.M. Shkol'nik, and K.K. Zabello, "Current density on the cathode of high current vacuum arc stabilized by axial magnetic field," in Proc. XIX ISDEIV, Xi'an, China, 2000, vol. 1, pp.286-289.
- [17] A.M. Chaly, I.N. Poluyanova, V.N. Polyyanov, "Maximum interrupting capacity of CuCr contacts under AMF", XXI ISDEIV, Yalta, Ukraine, 2004.